J Fluoresc (2009) 19:747–753
DOI 10.1007/s10895-009-0471-1

ORIGINAL PAPER

An Evaluation of a Fluorometric Method for Determining Binding Parameters of Drug–Carrier Complexes Using Mathematical Models Based on Total Drug Concentration

Boontarika Chanvorachote · Ubonthip Nimmannit · Walaisiri Muangsiri · Lee Kirsch

Received: 19 September 2008 / Accepted: 10 February 2009 / Published online: 8 April 2009

Abstract A fluorescence method for determining the mode of binding and estimating binding parameters in a model drug-carrier complex was developed using the lipopeptide antibiotic daptomycin and polyamidoamine (PAMAM) dendrimer. Mathematical simulations of model equations describing fluorescence changes induced by antibiotic–carrier binding in terms of total drug concentration were used to evaluate the sensitivity of parameter variation on binding isotherms for both one- and two-site binding models. Nonlinear regression analysis was used to estimate binding parameters and to identify pH-dependent binding models.

Keywords Fluorescence methods · Drug binding · Dissociation constant · Capacity constant · and Drugcarrier complexes

Introduction

Fluorescence spectroscopy has been used to evaluate binding phenomena in systems containing fluorophores whose spectral properties are altered in response to the intermolecular interaction [5, 8, 18]. Typically these changes are due to alterations of microenvironment of the fluorophore that causes quenching [3, 13, 17] or enhancement [6, 12].

B. Chanvorachote · U. Nimmannit · W. Muangsiri
Faculty of Pharmaceutical Science, Chulalongkorn University, Bangkok, Thailand

L. Kirsch (✉)
Division of Pharmaceutics, College of Pharmacy, The University of Iowa, Iowa City, IA 52242, USA
e-mail: lee-kirsch@uiowa.edu

Mathematical models describing equilibrium binding systems are typically presented in term of free ligand concentration rather than total concentration [9]. The use of these model equation are therefore restricted to the cases in which either the bound concentration are much smaller than the total concentration, so that the concentrations of free ligand can be equated to their total concentration, or the free concentration can be determined [1, 10]. However, these conditions are not always met when spectral methods are used as binding probes. To overcome this limitation, equations have been derived estimating for affinity and capacity constants using fluorescence titration data wherein the total ligand concentration is known, but not the bound and free concentrations. We have evaluated the use of these model equations in selecting the appropriate binding model and estimating binding parameters using an exemplary drug-carrier complex between antibiotic drug daptomycin and polyamidoamine (PAMAM) dendrimers [2, 15, 16].

Daptomycin contains two aromatic residues (tryptophan and kynurenine) that are intrinsically fluorescent. It is not surprising that conditions that alter daptomycin conformations may also cause fluorescence changes. Lakey and coworkers showed that the tryptophan emission of daptomycin is quenched by the absorption of kynurenine since tryptophan emission spectrum overlap with kynurenine absorption spectrum [6]. The quenching effect is based on the proximity of two fluorophores. Moreover, they observed that the kynurenine emission intensity is higher when kynurenine is a part of daptomycin than in the free amino acid form. The kynurenine fluorescence has been shown to be a sensitive probe for intermolecular interactions when used in steady-state fluorescence measurements. Lakey and Ptak studied the binding of daptomycin to 1,2-dimyristoyl-sn-glycero-3-phosphocholine (DMPC)

and dipalmitoyl phosphatidylcholine phospholipid (DPPC) [6, 7]. In the presence of calcium, a tenfold fluorescent enhancement and 15-nm blue shift was observed that was attributed to the penetration of daptomycin into the lipid bilayer.

The self-association of daptomycin has also been studied using steady-state fluorescence methods. A fluorescence enhancements and blue-shift were used to estimate pH-dependent critical aggregation concentrations (CAC). At pH 4, the lowest CAC value (0.1 mM) was observed [14].

Daptomycin-calcium ions association constants have been determined by circular dichroism (CD) spectroscopy [4]. Addition of liposomes composed of a one-to-one mixture of the zwitterionic phospholipid phosphatidyl coline (PC) and the acidic phospholipid phosphatidyl glycerol (PG) in the present of calcium was observed to induce an inversion of CD spectrum that indicated a substantial conformational change upon association with negatively charged membranes.

The interaction of daptomycin and fibrinogen has been studied using surface plasmon resonance [11]. The dissociation constant between daptomycin and fibrinogen were 4×10^{-6} M estimated using one-site binding model.

Methods

Chemicals

PAMAM dendrimer (generation 6) was purchased from Aldrich (USA). Daptomycin was obtained from Lilly Research Laboratories, Indianapolis, IN. All other chemicals were analytical grade or better. Double-distilled water was used throughout.

Fluorescence titrations

The PAMAM dendrimer received in methanol which was removed by evaporation using nitrogen gas. The residue was dissolved with double-distilled water to a concentration of 0.014 μM. Daptomycin-PAMAM dendrimer complex was formed by titration of five microliter aliquots of 74.0 μM aqueous daptomycin into 3 mL of PAMAM solution using a Hamilton syringe. Both dendrimer and daptomycin solutions were pH adjusted to either pH 4.0 or 7.0 prior to their addition. Buffers were not used and the pH value of mixtures did not vary by more than 0.1 pH units over the course of each titration. Titrations were conducted in a fluorescence quartz cell equipped with a magnetic stirrer. The final concentration of daptomycin was 4.6 μM and each titration was performed in triplicate. The mixture was stirred for 3 min after each addition. Fluorescence responses were measured using a Perkin Elmer LS-55 spectrofluorimeter. The excitation wavelength was set at tryptophan excitation wavelength (285 nm) and the emission spectra were scanned from 320 to 540 nm in order to observe the emission response from both tryptophan and kynurenine. Control studies were conducted by titration of aliquots of daptomycin to 3 mL of double-distilled water.

Results

Solutions containing PAMAM dendrimer showed no fluorescence emission maxima over the wavelength range of 320 to 540 nm. The addition of daptomycin aliquots into aqueous blank solutions (absence of dendrimer) resulted in a super imposable linear increase of fluorescence intensity with daptomycin concentration (≤5 μM) at both pH values of 4.0 and 7.0 (Fig. 1). No inflections were observed in these titrations which was important because daptomycin is known to form aggregates that result in fluorescence enhancements. The studies reported herein were intentionally conducted at daptomycin concentrations below the critical aggregation concentration [14].

The addition of daptomycin into dendrimer solution at both pH values of 4.0 and 7.0 resulted in significant increases fluorescence intensities at 460 nm (which corresponds to the peak maximum for kynurenine emission, Fig. 1). The concentration dependent fluorescence response profiles were non-linear and different at pH 4.0 and 7.0.

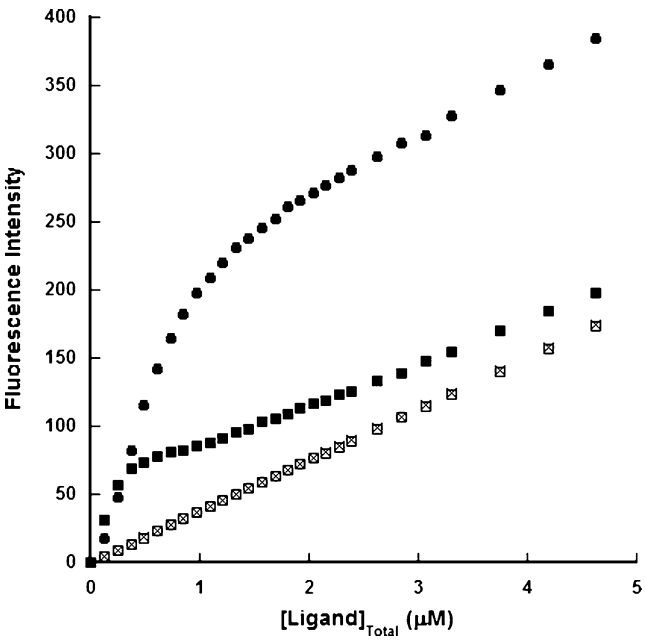

Fig. 1 Kynurenine fluorescence enhancement of daptomycin at 460 nm in the presence of PAMAM dendrimer generation 6 at pH 4.0 (*filled circle*) and 7.0 (*filled square*), and in the absence of PAMAM dendrimer generation 6 at pH 4.0 (*empty circle*) and 7.0 (*ex symbol*)

Fluorescence titration binding isotherms were constructed by plotting the difference in fluorescence intensity responses for equimolar daptomycin solutions in the presence and absence of dendrimer (ΔF, Fig. 2). The resulting isotherm for pH 4.0 titrations was biphasic wherein the ΔF values increased until a total daptomycin concentration of approximately 1.5 μM and then became independent of daptomycin concentration. Contrariwise, the pH 7.0 isotherm displayed increasing ΔF values up to daptomycin concentration of 0.4 μM whereupon ΔF values decreased with subsequent additions of titrant. These results suggested pH-dependent differences in daptomycin-dendrimer interactions both in the mode and values of the binding parameters. The exact nature of this binding phenomenon will be presented in a future manuscript; the issue to be resolved herein is the development of a method for reliably determining the mode of interaction and accurately determining the values for binding parameters from fluorescence titration data.

Discussion

Development of fluorescence titration binding models

The method for using fluorescence titration data in combination with the total ligand concentration to determine the mode of binding and estimating the binding parameters was adapted from the work of Wang and Jiang [19]. In the ensuring discussion, model equations are presented for estimating binding parameters associated with one- and two-site binding models and the effects of parameter variation on the shapes of the isotherms is evaluated by model simulation and by comparison to exemplary daptomycin-dendrimer data to determine whether the model equations adequately describe the fluorescence titration isotherms.

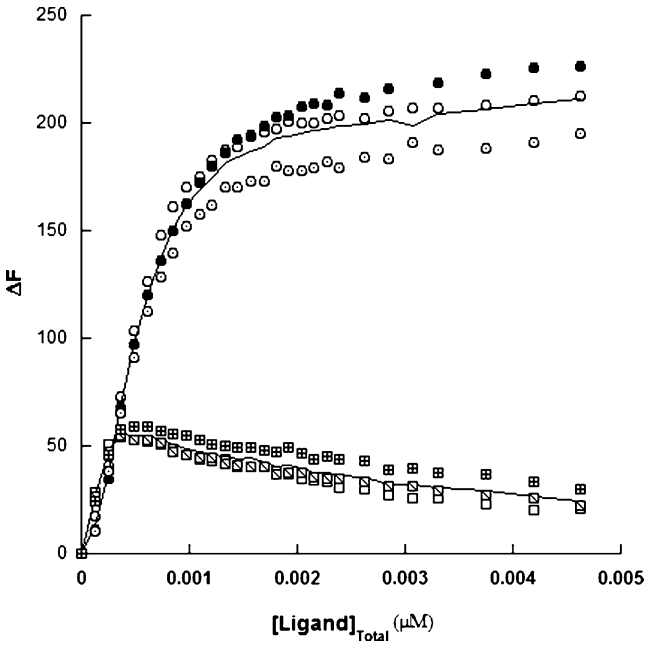

Fig. 2 Binding isotherm of the interaction between PAMAM generation 6 and daptomycin at pH 4.0 (*circle*) and 7.0 (*square*) at 25 °C

One-site binding model

For a single site binding model, the equilibrium dissociation constant (K_d) and molar ratio of bound drug to carrier molecule (r) is given by Eqs. 1 and 2:

$$K_d = \frac{[\text{Carrier}]_F \times [\text{Drug}]_F}{[\text{Drug}]_B} = \frac{([\text{Carrier}]_T - [\text{Drug}]_B) \times [\text{Drug}]_F}{[\text{Drug}]_B} \tag{1}$$

where $[\text{Carrier}]_F$, $[\text{Carrier}]_T$, $[\text{Drug}]_F$ and $[\text{Drug}]_B$ represent the concentration of free carrier, total carrier, free drug, and bound drug, respectively.

$$r = \frac{[\text{Drug}]_B}{[\text{Carrier}]_T} = \frac{[\text{Drug}]_F}{K_d + [\text{Drug}]_F} \tag{2}$$

The molar concentration of bound drug is given by Eq. 3 where R is the total number of independent binding sites $\left(R = n \times [\text{Carrier}]_T\right)$ and n is the number of independent sites on each carrier molecule.

$$[\text{Drug}]_B = \frac{R \times [\text{Drug}]_F}{K_d + [\text{Drug}]_F} \tag{3}$$

If the drug contains a fluorophore whose spectral properties change upon binding then the resulting fluorescence intensity change (ΔF) is given by Eq. 4 where ΔE represents the difference in molar extinction between the free and bound fluorophore.

$$\Delta F = \Delta E \times [\text{Drug}]_B = \Delta E \times \frac{R \times [\text{Drug}]_F}{K_d + [\text{Drug}]_F} \tag{4}$$

The free drug concentration in Eq. 3 can be described by mass balance in terms of the bound and total drug concentrations which allows for the derivation of a quadratic equation that describes the bound drug concentration in terms of the total drug concentration as shown in Eq. 5.

$$[\text{Drug}]_B = \frac{1}{2} \left\{ \left([\text{Drug}]_T + K_d + R\right) \pm \sqrt{\left([\text{Drug}]_T + K_d + R\right)^2 - 4 \times R \times [\text{Drug}]_T} \right\} \tag{5}$$

Substitution of Eq. 5 into Eq. 4 yields Eq. 6 which describes the change in fluorescence signal in terms of the

total drug concentration, binding parameters (K_d and R) and molar extinction changes.

$$\Delta F = \frac{\Delta E}{2} \left\{ ([\text{Drug}]_T + K_d + R) \pm \sqrt{([\text{Drug}]_T + K_d + R)^2 - 4 \times R \times [\text{Drug}]_T} \right\} \quad (6)$$

Experimentally, the value for ΔF is determined by the difference in fluorescence signals between equimolar solutions of drug in the presence and absence of carrier. Titration experiments can be used to generate fluorescence isotherms wherein the binding and molar extinction parameters can be estimated by nonlinear regression.

Properties of Eq. 6 were investigated by simulation using various values for the three adjustable model parameters: molar signal coefficient (ΔE=120 to 360), dissociation constant (K_d=0.06 to 0.18 μM^{-1}) and the total number of independent binding sites (R=0.55 to 1.45). The simulations were compared to the pH 4.0 daptomycin-dendrimer fluorescence titration data.

In the first series of simulations (Fig. 3), the effects of varying ΔE (120 to 360) on the fluorescence titration isotherm caused an amplitude variation of each ΔF value without changing the overall shape of the isotherm. Contrariwise, decreases in dissociation constant values (K_d=0.18 to 0.06 μM^{-1}) resulted in increased slope values in the ascending portion of the titration profile (Fig. 4). And

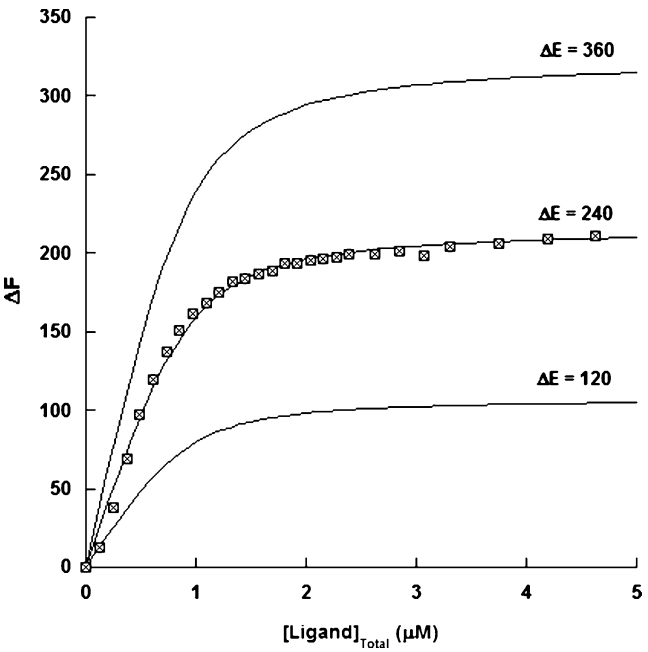

Fig. 3 Simulation plots of one-site binding model equations showing the effect of the molar signal coefficient variation (ΔE=120 to 360) are compared to the average binding isotherm values for PAMAM generation 6 and daptomycin at pH 4.0 (⊠)

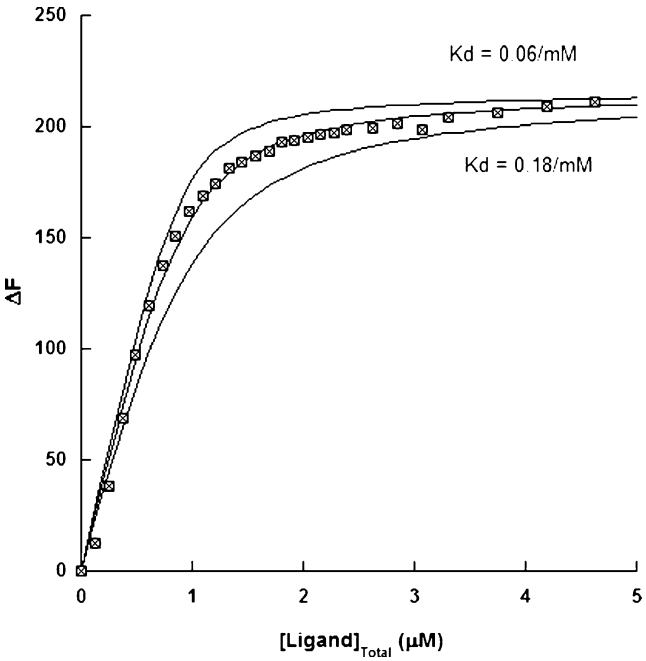

Fig. 4 Simulation plots of one-site binding model equations showing the effect of the dissociation constant variation (K_d=0.06 to 0.18 μM^{-1}) are compared to the average binding isotherm values for PAMAM generation 6 and daptomycin at pH 4.0 (⊠)

increased values for binding capacities (R=0.55 to 1.45) changed the maximum value of ΔF without effecting the ascending slope (Fig. 5). Thus a unique set of estimated parameter values was necessary to provide a complete description of the daptomycin-dendrimer data. Moreover

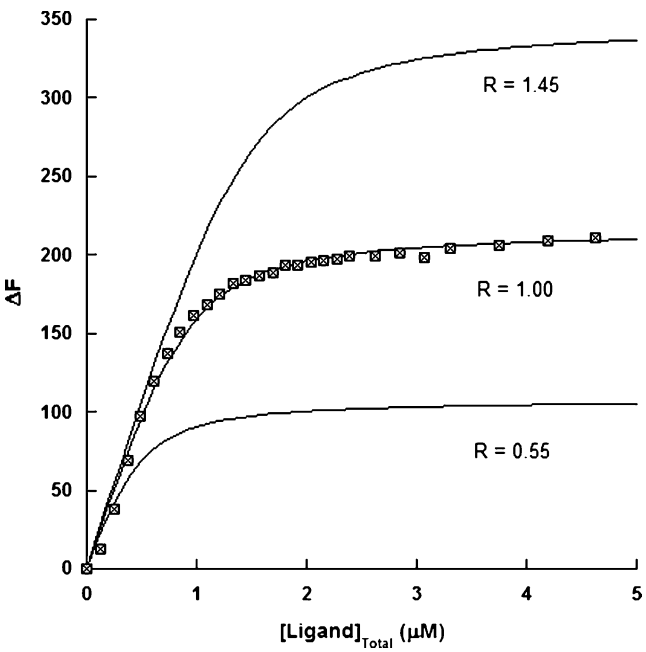

Fig. 5 Simulation plots of one-site binding model equations showing the effect of variation in the total number of independent binding sites (R=0.55 to 1.45) are compared to the average binding isotherm values for PAMAM generation 6 and daptomycin at pH 4.0 (⊠)

the shape of the fluorescence titration isotherm was consistent the simulated profile shapes using the one-site model.

A typical experimental data set is also depicted using the average values of triplicate titrations of PAMAM dendrimer generation 6 with daptomycin at pH 4.0. The good agreement between experimental data and model simulations demonstrates the usefulness of the fluorescence titration equations for one-site binding model applications.

Two-site binding model

The same approach was used to derive fluorescence titration equations for a two-site binding model wherein the concentration of bound molecules is given by

$$[\text{Drug}]_B = \frac{R_1 \times [\text{Drug}]_F}{K_{d1} + [\text{Drug}]_F} + \frac{R_2 \times [\text{Drug}]_F}{K_{d2} + [\text{Drug}]_F} \quad (7)$$

and K_{d1}, R_1 and K_{d2}, R_2 are the dissociation constants and the total number of each independent sites for the two independent binding sites. In this case, a cubic expression of free drug concentration was derived and used with Eq. 7 to derive Eq. 8 which describes the change in fluorescence signal between equimolar concentrations of drug in the presence and absence of carrier in terms of the molar

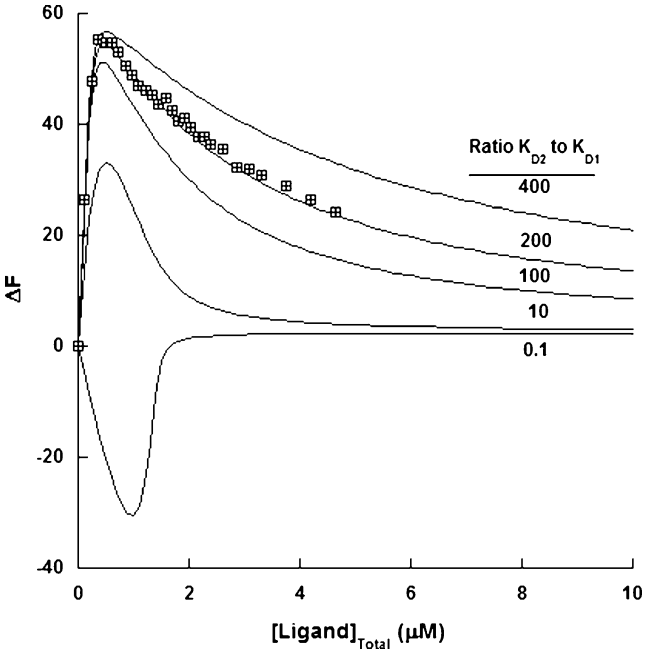

Fig. 7 Simulation plots of two-site binding model equations showing the effect of variation in the ratios of second and first site dissociation constants (K_{d2}/K_{d1}=0.1 to 400) are compared to the average binding isotherm values for PAMAM generation 6 and daptomycin at pH 7.0 (⊞)

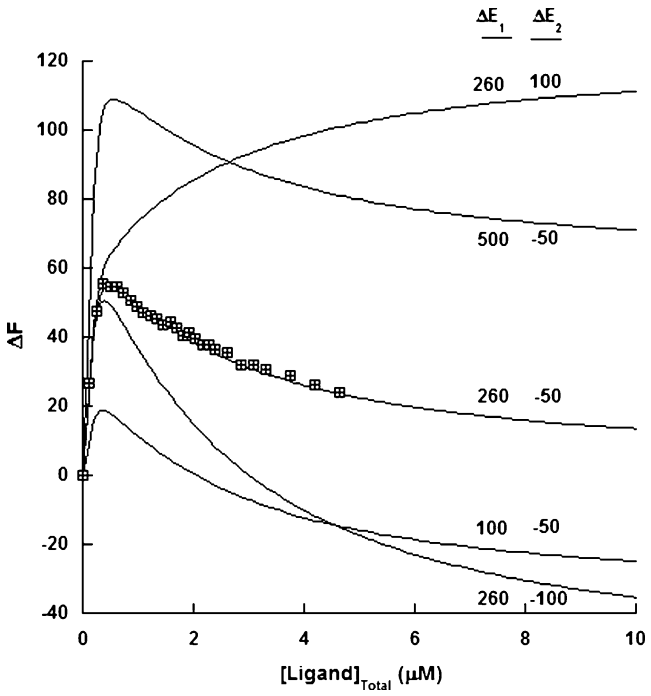

Fig. 6 Simulation plots of two-site binding model equations showing the effect of variation in the molar signal coefficients for two independent binding sites (ΔE_1=100 to 500, and ΔE_2= −100 to 100) are compared to the average binding isotherm values for PAMAM generation 6 and daptomycin at pH 7.0 (⊞)

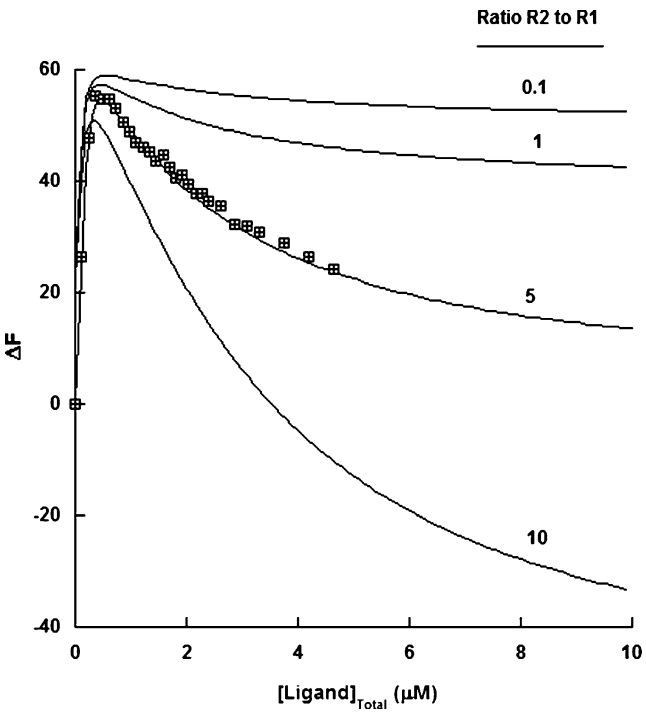

Fig. 8 Simulation plots of two-site binding equation showing the effect of variation in the ratios of the total number of second and first sites (R_2/R_1=0.1 to 10) are compared to the average binding isotherm values for PAMAM generation 6 and daptomycin at pH 7.0 (⊞)

extinction parameters, total drug concentration and binding parameters.

$$\Delta F=\Delta E_1 \times \left(\frac{R_1 \times [\text{Drug}]_F}{K_{d1}+[\text{Drug}]_F}\right)+\Delta E_2 \times \left(\frac{R_2 \times [\text{Drug}]_F}{K_{d2}+[\text{Drug}]_F}\right) \quad (8)$$

where $[\text{Drug}]_F$, a, b, c and θ are given by the following relationships and are defined in terms of binding parameters and the total drug concentration.

$$\begin{aligned}
[\text{Drug}]_F &= -\tfrac{a}{3}+\tfrac{2}{3}\sqrt{(a^2-3b)}\cos\tfrac{\theta}{3}\\
a &= K_{d1}+K_{d2}+R_1+R_2-[\text{Drug}]_T\\
b &= K_{d1}K_{d2}+K_{d2}R_1+K_{d1}R_2-(K_{d1}+K_{d2})[\text{Drug}]_T\\
c &= -K_{d1}K_{d2}[\text{Drug}]_T\\
\theta &= \arccos\frac{-2a^3+9ab-27c}{2\sqrt{(a^2-3b)^3}} \quad (0<\theta<\pi)
\end{aligned} \quad (9)$$

Once again, the binding and fluorescence parameters can be estimated from titration experiments wherein the fluorescence changes at equimolar drug concentrations (in the presence and absence of carrier) are plotted as a function of total drug concentration.

A series of simulations using two-site binding model equations were conducted by varying ΔE_1 (100–500) and ΔE_2 (−100–100) independently and by varying the ratios of K_{d2}/K_{d1} (0.1–400) and R_2/R_1 (0.1–10). Nearly all of the titration profiles were biphasic involving an ascending and descending portion except in the single simulation wherein both ΔE_1 and ΔE_2 had positive values. Varying ΔE_1 (Fig. 6) resulted in an amplitude effect on each of the ΔF values in both the ascending and descending phases. Varying ΔE_2 affected the ΔF values in the higher concentration portion of the titration profile (Fig. 6). The simulation in which both ΔE_1 and ΔE_2 had positive values illustrates a two-site titration curve wherein ligand binding at both sites results in fluorescence enhancement. Clearly the shape differences between this titration curve and a titration curve resulting from a one-site model are subtle.

The effect of varying the affinity of ligand for the two independent sites is illustrated in Fig. 7. In all of these simulations the value of K_{d1} was constant so the main effects were observed in the descending profile: at higher concentrations wherein the high affinity sites (K_{d1}) are saturated. A dissociation constant ratio of 400 implies that the binding affinity at the second site is many times less than at the high affinity site. Nonetheless the descending profile provided clear evidence for a second site. The bottom profile in Fig. 7 illustrates the expected titration profile when the higher affinity site is associated with a decrease in fluorescence.

The effect of varying the second site capacity constant is illustrated in Fig. 8. Again the major effects were observed in the descending portion of the titration profile. Under the conditions of the simulations, a low capacity second site R_2/R_1=0.1) would be difficult to distinguish from a single site binding model.

A typical experimental data set is also depicted using the average values of triplicate titrations of PAMAM dendrimer generation 6 with daptomycin at pH 7.0. The agreement between these data and two-site model simulations using the best estimates for each of the model parameters was good. Variations in any of the parameter produced titration profiles that were clearly different from these exemplary data. This result provides visual evidence for the utility of the fluorescence titration model equations in selecting an appropriate binding model and accurately estimating binding parameters.

Nonlinear regression analysis for estimation of the binding parameters

In this study, the nonlinear regression was performed using WinNonlin (software version 5.0.1, Pharsight Corporation). For the experimental data set obtained from the average values of triplicate titrations of PAMAM dendrimer generation 6 with daptomycin at pH 4.0, curve fitting using one-site binding equation appeared to completely describe the experimental data. The estimated values of ΔE, K_d and R were 239.45, 0.12 mM^{-1}, and 0.90, respectively. The two-site binding equation was used to describe the experimental data set obtained from the average values of triplicate titrations of PAMAM dendrimer generation 6 with daptomycin at pH 7.0. The model-predicted isotherms agree well with the experimental data, and the estimated values of ΔE_1, ΔE_2, K_{d1}, K_{d2}, R_1 and R_2 were 259.73, −49.70, 0.01 mM^{-1}, 2.00 mM^{-1}, 0.24, and 1.22, respectively. These results demonstrate the pH-dependent differences in daptomycin-dendrimer interactions both mode of binding and the binding parameters values. The nature of these differences and their implications for describing the mechanisms of daptomycin-dendrimer binding will be presented in a future manuscript.

References

1. Conners A (1987) Binding constants, the measurement of molecular complex stability. Wiley, New York
2. Cryan S-A (2005) Carrier-based strategies for targeting protein and peptide drugs to the lungs. AAPS J 07(01):E20–E41 doi:10.1208/aapsj070104
3. Epps E, Raub TJ, Caiolfa V, Chiari A, Zamai M (1999) Determination of the affinity of drugs toward serum albumin by measurement of the quenching of the intrinsic tryptophan

fluorescence of the protein. J Pharm Pharmacol 51(1):41–48 doi:10.1211/0022357991772079
4. Jung D, Rozek A, Okon M, Hancock REW (2004) Structural transitions as determinants of the action of the calcium-dependent antibiotic daptomycin. Chem Biol 11:949–957 doi:10.1016/j.chembiol.2004.04.020
5. Klajnert B, Pastucha A, Shcharbin D, Bryszewska M (2007) Binding properties of polyamidoamine dendrimers. J Appl Polym Sci 103:2036–2040 doi:10.1002/app.25279
6. Lakey JH, Ptak M (1988) Fluorescence indicates a calcium-dependent interaction between the lipopeptide antibiotic LY146032 and phospholipid membranes. Biochemistry 27:4639–4645 doi:10.1021/bi00413a009
7. Lakey JH, Maget-Dana R, Ptak M (1989) The lipopeptide antibiotic A21978C has a specific interaction with DMPC only in the presence of calcium ions. Biochim Biophys Acta 985:60–66 doi:10.1016/0005-2736(89)90104-1
8. Lakowicz R (2006) Principles of fluorescence spectroscopy, 3rd edn. Springer, Berlin
9. Larsson Å (1997) Regression analysis of simulated radio-ligand equilibrium experiments using seven different mathematical models. J Immunol Methods 206(1–2):135–142
10. Liu HL, Liang KH, Xu LL, Tong B (2007) Tang: Supramolecular interaction of ethylenediamine linked beta-cyclodextrin dimer and berberine hydrochloride by spectrofluorimetry and its analytical application. Talanta 74(1):140–145 doi:10.1016/j.talanta.2007.05.048
11. Muangsiri W, Kirsch LE (2006) The protein-binding and drug release properties of macromolecular conjugates containing daptomycin and dextran. Int J Pharm 315:30–43 doi:10.1016/j.ijpharm.2006.02.016
12. Okabe N, Hashizume N (1994) Drug binding properties of glycosylated human serum albumin as measured by fluorescence and circular dichroism. Biol Pharm Bull 17(1):16–21
13. Parikh HH, Mcelwain K, Balasubramanian V, Leung W, Wong D, Morrise ME, Ramanathan M (2000) A rapid spectrofluorimetric technique for determining drug-serum protein binding suitable for high-throughput screening. Pharm Res 17(5):632–637 doi:10.1023/A:1007537520620
14. Qiu J,, Kirsch LE (2007) Evaluation of lipopeptide aggregation (Daptomcyin) using light scattering, fluorescence, and NMR spectroscopy. AAPS J 9:S2
15. Rawat D, Singh S, Saraf S, Saraf S (2006) Nanocarriers: promising vehicle for bioactive drugs. Biol Pharm Bull 29 (9):1790–1798 doi:10.1248/bpb.29.1790
16. Svenson S, Tomalia DA (2005) Dendrimers in biomedical applications—reflections on the field B. Adv Drug Deliv Rev 57:2106–2129 doi:10.1016/j.addr.2005.09.018
17. Thomas P, Nelson G, Patonay G, Warner IM (1988) Analysis of drug binding sites on human serum albumin using multidimensional fluorescence measurements. Spectrochimica Acta 43B(4–5):651–660
18. Wang YP, Wei YL, Chuan D (2006) Study on the interaction of 3,3-bis(4-hydroxy-1-naphthyl)-phthalide with bovine serum albumin by fluorescence spectroscopy. J Photochem Photobiol Chem 177:6–11 doi:10.1016/j.jphotochem.2005.04.040
19. Wang Z-X, Jiang R-F (1996) A novel two-site binding equation presented in terms of the total ligand concentration. FEBS Lett 392:245–249 doi:10.1016/0014-5793(96)00818-6